Molecular and Cellular Endocrinology 584 (2024) 112160

Contents lists available at ScienceDirect

Molecular and Cellular Endocrinology

journal homepage: www.elsevier.com/locate/mce

PMM2 controls ERα levels and cell proliferation in ESR1 Y537S variant expressing breast cancer cells

Manuela Cipolletti, Filippo Acconcia *

Department of Sciences, Section Biomedical Sciences and Technology, University Roma Tre, Rome, Italy

ARTICLE INFO

Keywords:
17β-estradiol
Estrogen receptor
PMM2
ESR1 mutation
Metastatic breast cancer

ABSTRACT

Purpose: Metabolic reprogramming in breast cancer (BC) subtypes offers potential personalized treatment targets. Estrogen receptor α (ERα)-positive BC patients undergoing endocrine therapy (ET) can develop ET-resistant metastatic disease. Specific mutations, like Y537S in ERα, drive uncontrolled cell proliferation. Targeting mutant receptor levels shows promise for inhibiting growth in metastatic BC expressing ERα variants. Additionally, metabolic reprogramming occurs in ERα Y537S mutant cells. Consequently, we conducted a screen to identify metabolic proteins reducing intracellular levels of ERα Y537S and inhibiting cell proliferation.

Methods: Nine metabolic proteins were identified in a siRNA-based screen, with phosphomannose mutase 2 (PMM2) showing the most promise. We measured the impact of PMM2 depletion on ERα stability and cell proliferation in ERα Y537S mutant cells. Additionally, we tested the effect of PMM2 reduction on the hyperactive phenotype of the mutant and its proliferation when combined with metastatic BC treatment drugs.

Results: PMM2 emerged as a significant target due to its correlation with better relapse-free survival, overexpression in ERα-positive tumors, and its elevation in ERα Y537S-expressing cells. Depletion of PMM2 induces degradation of ERα Y537S, inhibits cell proliferation, and reduces ERα signaling. Notably, reducing PMM2 levels re-sensitizes ERα Y537S-expressing cells to certain ET drugs and CDK4/CDK6 inhibitors. Mechanistically, depletion of PMM2 leads to a reduction in *ESR1* mRNA levels, resulting in decreased ERα receptor protein expression. Furthermore, the reduction of PMM2 decreases FOXA1 levels, which plays a crucial role in ERα regulation.

Conclusions: Our findings establish PMM2 as an innovative therapeutic target for metastatic BC expressing the ERα Y537S variant, offering alternative strategies for managing and treating this disease.

1. Introduction

Breast cancer (BC) is a prevalent malignancy affecting women worldwide, but it should not be considered as a homogeneous disease entity. BC exhibits considerable heterogeneity and encompasses various phenotypes that can be categorized based on different diagnostic criteria. The most frequent BC subtype observed in patients is characterized by the expression of estrogen receptor alpha (ERα) and generally demonstrates a more favorable prognosis compared to ERα-negative tumors. Nonetheless, not all ERα-positive tumors are identical, as they can be further stratified based on the presence or absence of specific receptors such as progesterone receptor (PR) and HER2/Neu, or by utilizing a 50-gene signature known as PAM50. The latter approach identifies five distinct molecular intrinsic subtypes (luminal A, luminal B, HER2/Neu-enriched, basal-like, and normal-like), which exhibit varying combinations of ERα, PR, and HER2/Neu expression. Additionally, each BC subtype can also be characterized by its histological type (e.g., invasive ductal carcinoma, adenocarcinoma, etc.), which may or may not align with the aforementioned molecular phenotypes (Tsang and Tse, 2020). Finally, the evaluation of the genomic and transcriptomic architecture of BC has additionally revealed that this disease can be classified in 10 integrative clusters (Curtis et al., 2012). Consequently, BC should not be regarded as a singular disease, as each patient possesses a unique tumor type.

The heterogeneity observed in BC enables the implementation of tailored pharmacological therapies based on tumor classification. Typically, tumors positive for ERα are treated with endocrine therapy (ET) drugs, including aromatase inhibitors, 4OH-tamoxifen, and fulvestrant. These medications specifically target the ERα signaling pathway activated by the sex hormone 17β-estradiol (E2). Anti-estrogen

* Corresponding author. Department of Sciences, University Roma Tre, Viale Guglielmo Marconi, 446, I-00146, Rome, Italy.
E-mail address: filippo.acconcia@uniroma3.it (F. Acconcia).

https://doi.org/10.1016/j.mce.2024.112160
Received 28 June 2023; Received in revised form 27 November 2023; Accepted 12 January 2024
Available online 22 January 2024

treatment is administered for a period of 5–10 years following surgical tumor removal and has demonstrated efficacy in reducing mortality rates. However, a significant proportion (at least 50%) of patients undergoing ET develop resistance to these drugs, leading to relapse and the development of metastatic disease, often resulting in fatality (Lumachi et al., 2011).

One of the mechanisms contributing to ET resistance involves the selection of constitutively active point mutations in the ERα of tumor cells. These mutations render the cancer cells insensitive to ET drugs and promote uncontrolled cell proliferation (Busonero et al., 2019). Among various receptor variants, the most prevalent is the Y537 to S (Y537S) mutation. This specific amino acid substitution causes the apo ERα to adopt a conformation identical to that of the E2-bound ERα, conferring a hyperactive and resistant phenotype to the mutant receptor (Katzenellenbogen et al., 2018).

Consequently, there is ongoing research to identify novel drugs that specifically target the mutant ERα. Specifically, molecules that directly bind to the receptor variant and promote its degradation are being investigated for their potential in clinical applications to impede the progression of metastatic BC (Katzenellenbogen et al., 2018). Furthermore, we have previously reported a selection of Food and Drug Administration (FDA)-approved drugs that do not directly bind to the ERα but have the ability to induce its degradation by activating various cellular pathways (Bartoloni et al., 2022; Busonero et al., 2020; Cipolletti et al., 2021a; Pescatori et al., 2022). These drugs have also demonstrated the capability to inhibit the proliferation of cells expressing the Y537S ERα variant (Bartoloni et al., 2022; Busonero et al., 2020; Cipolletti et al., 2021a; Pescatori et al., 2022). This indicates that promoting the degradation of ERα is sufficient to hinder cell proliferation, regardless of the drug's ability to directly bind to the receptor (Busonero et al., 2019). Instead, the drugs act by targeting parallel cellular pathways that subsequently impact ERα stability through diverse mechanisms (Busonero et al., 2019).

The Y537S ERα variant expressing cells have been subjected to molecular characterization, revealing notable metabolic alterations. These cells exhibit enhanced mitochondrial metabolism (Fiorillo et al., 2018) and lipid metabolism (Martin et al., 2017; Du et al., 2018). Intriguingly, our recent investigation utilizing a siRNA-based screen for metabolic proteins in our anti-estrogen discovery platform (Cipolletti et al., 2021a) has identified GART, a tripartite enzyme involved in the second enzymatic step of the de novo purine biosynthetic pathway, as a significant factor. Inhibition of GART leads to ERα degradation and effectively hampers the proliferation of both luminal A invasive ductal carcinoma cell lines and cells expressing the Y537S ERα variant (Cipolletti et al., 2023).

Remarkably, during the same screen, we made an additional observation that reducing the levels of nine metabolic proteins (MARS, PMM2, AZIN2, GAD1, SLC27A4, CA4, CA14, FKBP6, PGAM2) selectively diminishes the expression of the Y537S ERα variant and impedes the proliferation of cells harboring this variant (Fig. 1). Consequently, the aim of this study was to validate and characterize the impact of these metabolic proteins on the stability of the Y537S ERα variant and its associated cell proliferation. Our data demonstrated that inhibiting PMM2 effectively prevents mutant receptor signaling, leading to impaired cell proliferation. Additionally, PMM2 inhibition sensitizes Y537S ERα mutant-expressing cells to clinically used drugs employed in the treatment of metastatic BC expressing this specific receptor point mutation.

2. Materials and Methods

2.1. Cell culture and reagents

MCF10a, MCF-7 were purchased by ATCC (USA) and maintained according to the manufacturer's instructions. DMEM (with and without phenol red), and fetal calf serum were purchased from Sigma-Aldrich (St. Louis, MO). Bradford protein assay kit, anti-mouse and anti-rabbit secondary antibodies, and chemiluminescence reagent for Western blot were obtained from Bio-Rad (Hercules, CA, USA). Antibodies against ERα (F-10, mouse), pS2 (A-10, mouse), cyclin D1 (A-12, mouse), caveolin-1 (N-20, rabbit), RARA (C-1, mouse), lamin B1 (Sc-374015, mouse) and cathepsin D (C-5, mouse) were obtained from Santa Cruz Biotechnology (Santa Cruz, CA, USA); anti-PMM2 (ab229996, rabbit), anti-BDNF (ab108319, rabbit) and anti-MARS (ab50793, mouse) antibodies were purchased by Abcam (Cambridge, UK). The antibody against FOXA1/HNF3α (53528S, rabbit) was purchased by Cell Signaling Technology (Danvers, MA, USA). Anti-vinculin (mouse) antibody was purchased from Sigma-Aldrich (St. Louis, MO, USA). Fulvestrant (i.e., ICI182,780) was purchased by Tocris (USA); cycloheximide (CHX), 4OH-Tamoxifen, esiRNA for PMM2, MARS and FOXA1 were purchased from Sigma-Aldrich (St. Louis, MO, USA). Palbociclib, abemaciclib, ribociclib, AZD9496 and GDC-0810 were purchased by Selleck Chemicals (USA). Promega (Madison, MA, USA) supplied the Nano-Glo® EndurazineTM. All the other products were from Sigma-Aldrich. Analytical- or reagent-grade products were used without further purification. The identities of all the used cell lines were verified by STR analysis (BMR Genomics, Italy).

2.2. Small Interference RNA

Cells were transfected with esiRNA against MARS or PMM2 and the procedure was carried out using Lipofectamine RNAi Max (Thermo Fisher) as previously reported (Cipolletti et al., 2023). Assays were performed 48 h after transfection.

2.3. Growth curves

Real-time cell analysis (RTCA) for time-dependent cell proliferation was conducted using the xCELLigence DP system from ACEA Biosciences, Inc. (San Diego, CA) Multi-E-Plate station, following previously reported methods (Pescatori et al., 2022). In this approach, the instrument measures the electrical impedance within each well and converts it into a cell index, which is directly proportional to the number of cells. The cell index is automatically normalized by the instrument at the time of drug administration. For co-administration analyses, drugs were administered at the specified times of cell plating, as indicated in the figure captions. For Crystal Violet staining, we performed cell number measurement as we did in (Pescatori et al., 2022).

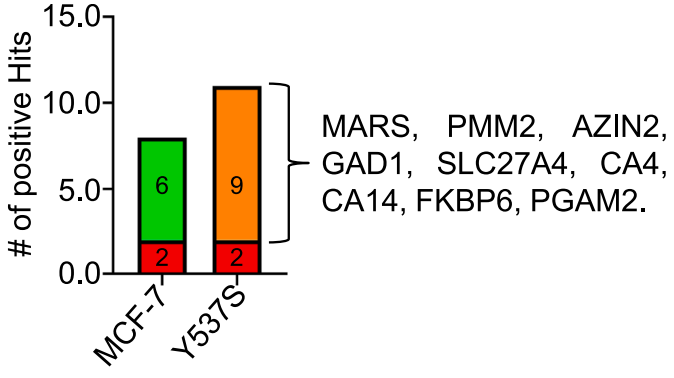

Fig. 1. Positive metabolic hits in MCF-7-Y537S cells.
Number of positive hit proteins in the metabolic screen described in (Cipolletti et al., 2023) for both MCF-7 (FROM ATCC) and MCF-7-Y537S cells. Red indicates the common proteins. Green indicates the number of proteins specifically affecting ERα levels and cell proliferation in MCF-7 (FROM ATCC) cells while orange indicates the number of proteins specifically affecting ERα levels and cell proliferation in MCF-7-Y537S. These latter proteins are then indicated via the bracket. For details, please see (Cipolletti et al., 2023).

2.4. Real-time measurement of NanoLucPest expression

MCF-7 cells and MCF-7-Y537S ERE-NLuc cells were seeded in 96-well plates at a density of 10,000 cells per well. Following siRNA-mediated transfection, the cells were incubated for 24 h, and the luciferase reaction was recorded as previously described. (Cipolletti et al., 2021b). MCF-7-Y537S ESR1-NLuc cells were generated and used as described in (Bartoloni et al., 2022).

2.5. Western blotting assays

To prepare cell lysates, the cells were lysed in YY buffer (containing 50 mM HEPES at pH 7.5, 10% glycerol, 150 mM NaCl, 1% Triton X-100, 1 mM EDTA, 1 mM EGTA), supplemented with protease and phosphatase inhibitors. For Western blotting analyses, 20–30 μg of protein was loaded onto SDS gels. The gels were then run and transferred to nitrocellulose membranes using the Biorad Turbo-Blot semidry transfer apparatus. Immunoblotting was performed by incubating the membranes with 5% milk for 60 min, followed by overnight incubation with the designated antibodies. The membranes were further incubated with secondary antibodies for an additional 60 min. Finally, the protein bands were visualized using a Biorad Chemidoc apparatus. Fractionation analyses were performed as previously described (Acconcia et al., 2007).

2.6. Gene array analyses

Total RNA was obtained from cells using TRIzol reagent (Invitrogen, Carlsbad, Ca, USA) following the manufacturer's guidelines. For gene expression analysis, the GoTaq 2-step RT-qPCR system (Promega, Madison, MA, USA) was employed for cDNA synthesis and qPCR. The ABI Prism 7900 HT Sequence Detection System (Applied Biosystems, Foster City, CA, USA) was used for this purpose, following the manufacturer's instructions. To analyze ERα target gene expression, the PrimePCR Estrogen receptor signaling (SAB Target List) H96 panel (Bio-Rad Laboratories, Hercules, CA, USA) was utilized for RT-qPCR-based gene array analysis, as per the manufacturer's instructions. The gene expression data was normalized to the levels of GAPDH mRNA present in the array. Genes were considered affected by PMM2 depletion if their fold induction was above 2.0 or below 0.7 compared to the control sample.

2.7. Statistical analysis

Statistical analysis was conducted using the Student's *t*-test. The InStat version 3 software system (GraphPad Software Inc., San Diego, CA) was utilized for this analysis. Densitometric analyses were carried out using the freeware software Image J by measuring the intensity of the protein of interest's band in relation to the intensity of the loading control band (vinculin). Significance was determined by *p* values, which are indicated in the corresponding figure legend.

3. Results

3.1. Breast cancer progression as a function of metabolic proteins

Initial experiments aimed to elucidate the potential significance of nine metabolic proteins (MARS, PMM2, AZIN2, GAD1, SLC27A4, CA4, CA14, FKBP6, PGAM2) in the progression of BC (Fig. 1 and Supplementary Fig. 1). To accomplish this, Kaplan-Meier plots were obtained from the Kaplan-Meier Plotter database (https://kmplot.com/analysis/) (Lanczky and Gyorffy, 2021). The plots were utilized to assess the relapse-free survival (RFS) of patients with BC, categorized as either ERα-positive or ERα-negative, in relation to the expression levels of the aforementioned metabolic proteins. The analysis revealed that only low levels of MARS and PMM2 mRNA were significantly associated with an increased probability of RFS in women with ERα-positive breast tumors. However, no significant differences in the RFS rate were observed in ERα-negative BC patients based on MARS2 mRNA levels, and a diminished significant difference was noted in the survival probability in relation to PMM2 levels (Fig. 2A–D and Supplementary Table 1). Interestingly, the RFS probability of women expressing varying mRNA levels of the other metabolic proteins was not significant in ERα--negative BC cases. Conversely, in patients with ERα-positive tumors, the difference in survival rates was either insignificant or a better RFS was observed in those with high mRNA levels of the protein (Supplementary Figs. 1 and 2 and Supplementary Table 2).

Given these findings, which suggest a potential role of MARS and PMM2 expression in ERα-positive BC progression, we decided to focus on PMM2 and MARS and subsequently, we assessed their mRNA expression in breast tumors compared to normal breast epithelium. The data obtained from the TNM plot (https://tnmplot.com/analysis/) (Bartha and Gyorffy, 2021) indicated that breast tumors exhibited higher levels of MARS and PMM2 mRNA compared to their normal counterparts (Fig. 2E and Supplementary Table 2). Since these metabolic proteins were identified in a screen utilizing a cellular system mimicking metastatic BC (i.e., MCF-7-Y537S) (Harrod et al., 2017), we further explored whether the expression of these proteins correlated with disease aggressiveness. To address this, the METABRIC datasets provided by the cBioPortal database (https://www.cbioportal.org/) (Cerami et al., 2012; Gao et al., 2013) were examined, revealing that both MARS and PMM2 mRNA expression levels were higher in grade 3 ERα-positive tumors and stage 3–4 tumors compared to grade 1 and stage 1–2 tumors (Fig. 2F and Supplementary Tables 3 and 4).

Collectively, these findings indicate that the expression of both MARS and PMM2 may contribute to the progression of ERα-positive BC.

3.2. PMM2 but not MARS protein expression correlates with ERα both in tumors and in BC cell lines and is upregulated in MCF-7-Y537S cells

Subsequently, we aimed to determine which of the two identified metabolic proteins may have a greater impact on the progression of BC. To accomplish this, we assessed the protein expression levels of MARS, PMM2, and ERα in relation to each other in breast tumors and various BC cell lines. To this end, we examined the Breast Cancer proteome, proteogenomic, and metabolomics landscape (https://www.breastcancerlandscape.org/) (Johansson et al., 2019), as well as the BC cell lines profiled in the DepMap portal (https://depmap.org/portal). Notably, a significant linear correlation was observed between PMM2 and ERα protein expression in breast tumors (Fig. 3A and Supplementary Table 5; $r = 0.3978$, $p = 0.0091$) and BC cell lines (Fig. 3C and Supplementary Table 6; $r = 0.4538$, $p = 0.0153$). However, no correlation was observed between MARS and ERα protein expression in both BCs and BC cell lines (Fig. 3B and Supplementary Table 5; Fig. 2D and Supplementary Table 6). Consistently, PMM2 protein expression was increased in ERα--positive tumors (Fig. 3E) and BC cell lines (Fig. 3F and Supplementary Table 6), while MARS protein expression was upregulated in ERα--negative tumors (Fig. 3E) and remained unchanged in ERα-positive and ERα-negative BC cell lines (Fig. 3F and Supplementary Table 6).

Next, we evaluated PMM2 mRNA expression in cell lines representing primary BC (i.e., MCF-7 cells) and metastatic BC resistant to endocrine therapy drugs (i.e., MCF-7-Y537S cells) (Harrod et al., 2017; Dai et al., 2017; Neve et al., 2006), by assessing the Affymetrix-based basal gene expression profiles in both cell lines (Busonero, 2018). Interestingly, PMM2 mRNA was upregulated in MCF-7-Y537S cells compared to MCF-7 cells (Fig. 3G and Supplementary Table 7). Notably, TFF1 was used as a positive control, as its expression is known to be increased in MCF-7-Y537S cells as reported elsewhere (Martin et al., 2017; Harrod et al., 2017, 2022). In contrast, no significant differences in MARS mRNA expression were detected between these two cell lines. Consistent with the previous findings, we also observed higher levels of both MARS and PMM2 proteins in MCF-7 and MCF-7-Y537S cells compared to

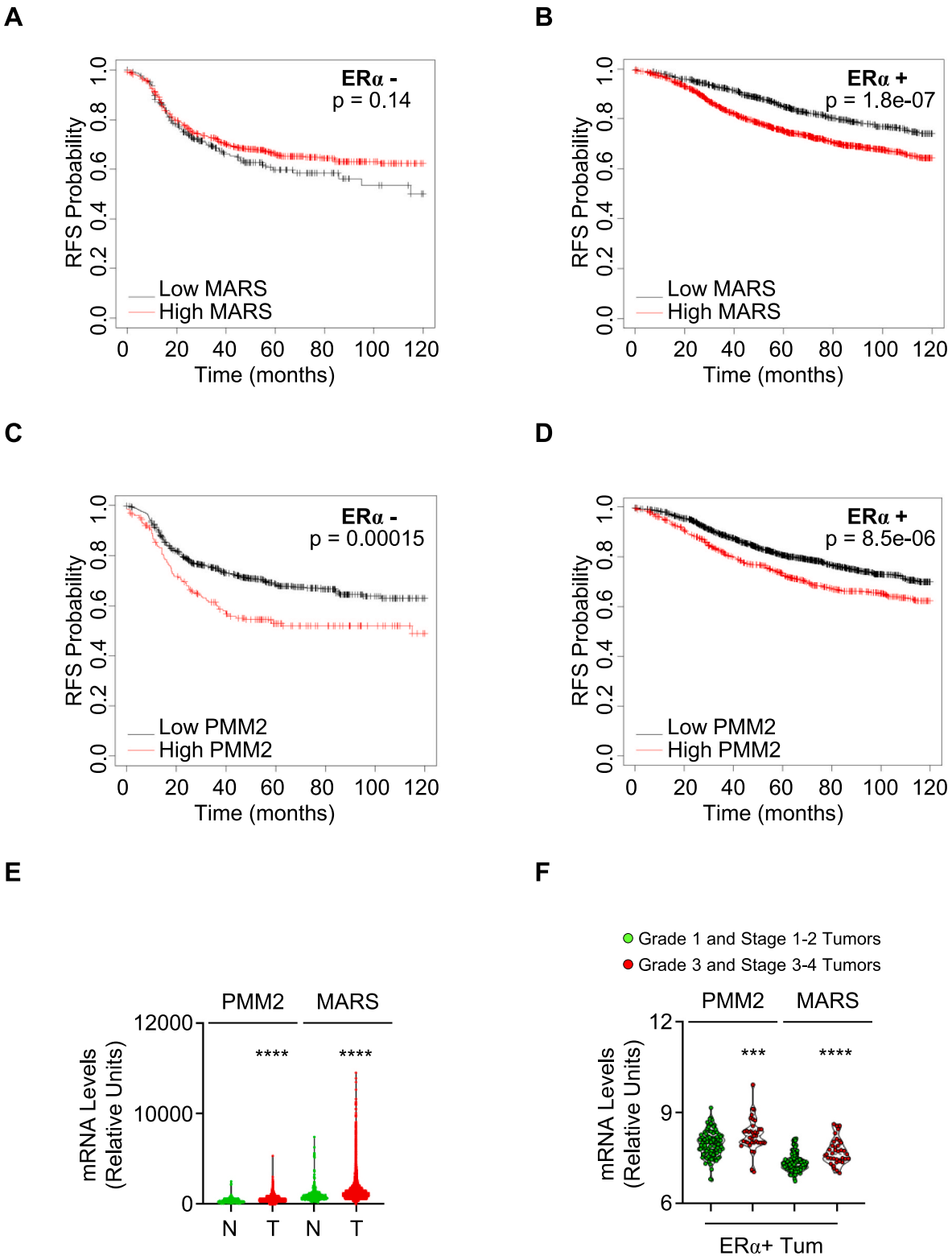

Fig. 2. The role of MARS and PMM2 in breast cancer progression.
Kaplan-Meier plots demonstrate the probability of relapse-free survival (RFS) in women with ERα-negative (A and C) or ERα-positive (B and D) breast cancer based on mRNA levels of MARS (A and B) or PMM2 (C and D). The cutoff values between the lower and upper quartiles are automatically determined, selecting the best-performing threshold (Lanczky and Gyorffy, 2021). The p-value indicating significant differences in RFS is provided for each panel. (E) Comparison of PMM2 and MARS mRNA levels between breast tumors and normal breast epithelium obtained from the TNM plot database (https://tnmplot.com/analysis/) (Bartha and Gyorffy, 2021). Significant differences ($p < 0.0001$) are denoted by ****, as determined by the Student t-test. (F) Relationship between MARS and PMM2 mRNA levels in breast cancer, considering the grade and stage of the disease using data from the cBioPortal database. Each dot represents a tumor. Significant differences ($p < 0.0001$) are denoted by ****, as calculated by the Student's t-test.

MCF10a cells, which serve as a model of normal breast epithelium (Dai et al., 2017; Neve et al., 2006; Soule et al., 1990). Additionally, only PMM2 protein expression was significantly increased in MCF-7-Y537S cells compared to MCF-7 cells (Fig. 3H, 3H′, and 3H'').

Taken together, these findings indicate a positive correlation between PMM2 and ERα expression in ERα-positive tumors as well as in BC cell lines. Moreover, protein levels of PMM2 are elevated in both ERα-positive tumors and BC cell lines. Furthermore, PMM2 is found to be overexpressed in MCF-7-Y537S cells.

3.3. PMM2 depletion reduces ERα levels and cell proliferation in MCF-7 and MCF-7-Y537S cells

Based on the previous findings, subsequent experiments were conducted to confirm the capacity of PMM2 to impact the stability of ERα and cell proliferation in MCF-7-Y537S cells (Cipolletti et al., 2023). It is important to note that MCF-7 cells were also included as a control cell line in these experiments.

In both MCF-7 and MCF-7-Y537S cells, depletion of PMM2 using siRNA resulted in a reduction in intracellular abundance of ERα (Fig. 4A–C). It is worth noting that while the extent of PMM2 depletion was similar in both cell lines, the reduction in receptor level was significantly more pronounced in MCF-7-Y537S cells compared to MCF-7 cells. Additionally, parallel experiments were conducted to investigate the impact of PMM2 on the proliferation of both MCF-7 and MCF-7-Y537S cells. For this purpose, the efficacy of PMM2 depletion was assessed by Western blotting (WB) analyses at the time of cell plating (insets in Fig. 4D and E), followed by monitoring cell proliferation for three days. As depicted in Fig. 4D and E, cells with reduced PMM2 expression exhibited decreased proliferation compared to control cells. However, consistent with previous findings, PMM2 depletion had a greater impact on the proliferation rate of MCF-7-Y537S cells compared to MCF-7 cells. To confirm the effect of PMM2 on cell proliferation, we also repeated the experiments by using the Crystal Violet staining as a classic method to measure the cell number in the same above-mentioned experimental conditions. As shown in Fig. 4F and F', depletion of PMM2 reduced the cell number only in MCF-7-Y537S cells. Notably, the differences observed in the two methods can be ascribed to a different sensibility of the xCelligence apparatus with respect to the Crystal Violet staining. However, these findings provide further validation for the observation that PMM2 depletion causes a significantly bigger reduction in ERα levels and cell proliferation in MCF-7-Y537S than in the parental MCF-7 cells (Cipolletti et al., 2023).

3.4. The impact of PMM2 depletion on ERα signaling in MCF-7-Y537S cells

The Y537S point mutation in ERα results in hyperactivation of the receptor due to a conformational change induced by this amino acid variant (Katzenellenbogen et al., 2018). This conformational change mimics the structure of wild-type (wt) ERα bound to its cognate hormone E2, leading to increased E2-dependent transcriptional signaling and promoting cell proliferation (Katzenellenbogen et al., 2018). Consequently, we aimed to investigate the effect of PMM2 depletion on the signaling of the ERα Y537S variant. To assess the ERα Y537S mutant's ability to activate estrogen response element (ERE)-based transcriptional activity, we utilized MCF-7-Y537S cell lines that stably express a reporter construct with the ERE sequence in the promoter region controlling the nano-luciferase (NLuc) gene (Cipolletti et al., 2021b). As a control, we also used the MCF-7 ERE-NLuc cells (Cipolletti et al., 2020). In these engineered cell lines, siRNA-mediated depletion of PMM2 (Fig. 5A) resulted in a significant reduction in the ERα ability to activate the ERE-based promoter activity (Fig. 5B). Interestingly, the depletion of PMM2 determined a significantly greater effect in the reduction in ERα ERE-based promoter activity in MCF-7-Y537S cells than in MCF-7 cells (Fig. 5B). Therefore, we next focused only on the effect of PMM2 in MCF-7-Y537S cells.

The transcriptional activity of ERα extends beyond genes that contain the ERE sequence in their promoter regions (Acconcia et al., 2021). To gain a comprehensive understanding of PMM2's impact on gene expression, we examined the effect of PMM2 depletion on the expression of approximately 100 validated ERα target genes as we previously did (Cipolletti et al., 2021a; Bartoloni et al., 2020). After siRNA-mediated PMM2 depletion, we compared the mRNA expression of these genes at 48 h. Genes were considered modulated by PMM2 depletion if their expression levels were increased by at least 2.0-fold or decreased by at least 0.7-fold. As depicted in Fig. 4C, the majority of modulated genes (71%) in the array showed reduced expression following PMM2 protein reduction, while only 29% of the modulated genes were upregulated by PMM2 depletion. Interestingly, we also observed a decrease in *ESR1* mRNA levels. Consistent with these findings, the measurement of mRNA levels in MCF-7-Y537S cells with reduced PMM2 expression exhibited a significant reduction in *ESR1* mRNA levels (Fig. 5D). Accordingly, time course analysis of cycloheximide (CHX) administration in MCF-7-Y537S cells shows that this protein synthesis inhibitor reduces ERα levels in control cells while in the presence of PMM2 depletion CHX does not induce a further reduction in receptor intracellular content (Supplementary Fig. 3). These data suggest that PMM2 regulates receptor levels through a transcriptional mechanism. Additionally, based on the gene array experiments, we found that PMM2 depletion in MCF-7-Y537S cells led to decreased protein expression of pS2, CatD, CycD1, FOXA1, Cav1, and RARA, while increasing intracellular levels of BDNF (Fig. 5E and E′).

Collectively, these results demonstrate that PMM2 depletion impairs the ability of the ERα Y537S variant to regulate ERE-based transcriptional activity and E2-dependent gene expression.

3.5. Mechanism for the PMM2-depletion reduction in ERα signaling in MCF-7-Y537S cells

Reduction in ERα transcriptional activity and gene expression can be due to reduced receptor recruitment on the chromatin region. Therefore, we next investigated if PMM2 depletion could affect the amount of ERα located on the chromatin. To this purpose, we performed fractionation analyses of growing MCF-7-Y537S cells both in the presence and in the absence of the siRNA directed against PMM2. As shown in Fig. 6A, the ERα can be found both in the cytoplasm and in the chromatin fraction of the MCF-7-Y537S cells. Furthermore, as expected, PMM2 is found in the cytoplasm fraction, and lamin B1 is found in the nuclear fractions of the same cell line. Notably, the depletion of PMM2 in MCF-7-Y537S cells did not modify the overall distribution of the receptor on the chromatin fraction but it reduced the overall amount of the receptor distributed in all the prepared fractions (Fig. 6A). Therefore, the reduction in ERα transcriptional activity does not depend on a reduced receptor quantity on the chromatin.

Because PMM2 depletion reduces *ESR1* mRNA content in MCF-7-Y537S cells (Fig. 5D) and concomitantly also reduces the amount of FOXA1 (Fig. 5E), we next hypothesized that the reduction in ERα transcriptional activity due to the reduction in ERα levels could be ascribed to a reduced FOXA1-dependent ability to control *ESR1* mRNA transcription and ERα expression (Bernardo et al., 2010). To test this hypothesis, we generated an MCF-7-Y537S cell line stably expressing the FOXA1-specific enhancer of the *ESR1* promoter region (i.e., the genetic region in the ERα gene promoter required for FOXA1-dependent ERα expression) (Bartoloni et al., 2022; Wang et al., 2018) upstream to a nanoluciferase (NLuc)-PEST reporter gene (MCF-7-Y537S ESR1-NLuc cells) and tested the effect of the reduction in PMM2 intracellular levels. As expected, the depletion of FOXA1 (Fig. 6B lower right panel) reduced the basal *ESR1* promoter activity (i.e., FOXA1 activity) (Fig. 6B). More importantly, PMM2 depletion in MCF-7-Y537S ESR1-NLuc cells (Fig. 6B lower left panel) was also able to determine a significant reduction in the basal *ESR1* promoter activity (Fig. 6B).

Altogether these data indicate that the reduction in PMM2 intracellular levels determines a reduction in the levels of FOXA1 and a reduction in FOXA1 activity towards the enhancer in the ERα gene promoter required for FOXA1-dependent ERα expression.

3.6. Targeting PMM2 in association with 4OH-tamoxifen and CDK4/CDK6 inhibitor administration as a novel potential treatment option for metastatic BC

One consequence of the selection of the ERα Y537S variant in cells is the development of tumor cells that acquire resistance to ET drugs such as 4OH-tamoxifen (Tam) and fulvestrant (ICI182,280 - ICI) (Katzenellenbogen et al., 2018). Consequently, significant research efforts are being directed toward identifying novel treatments for metastatic BC

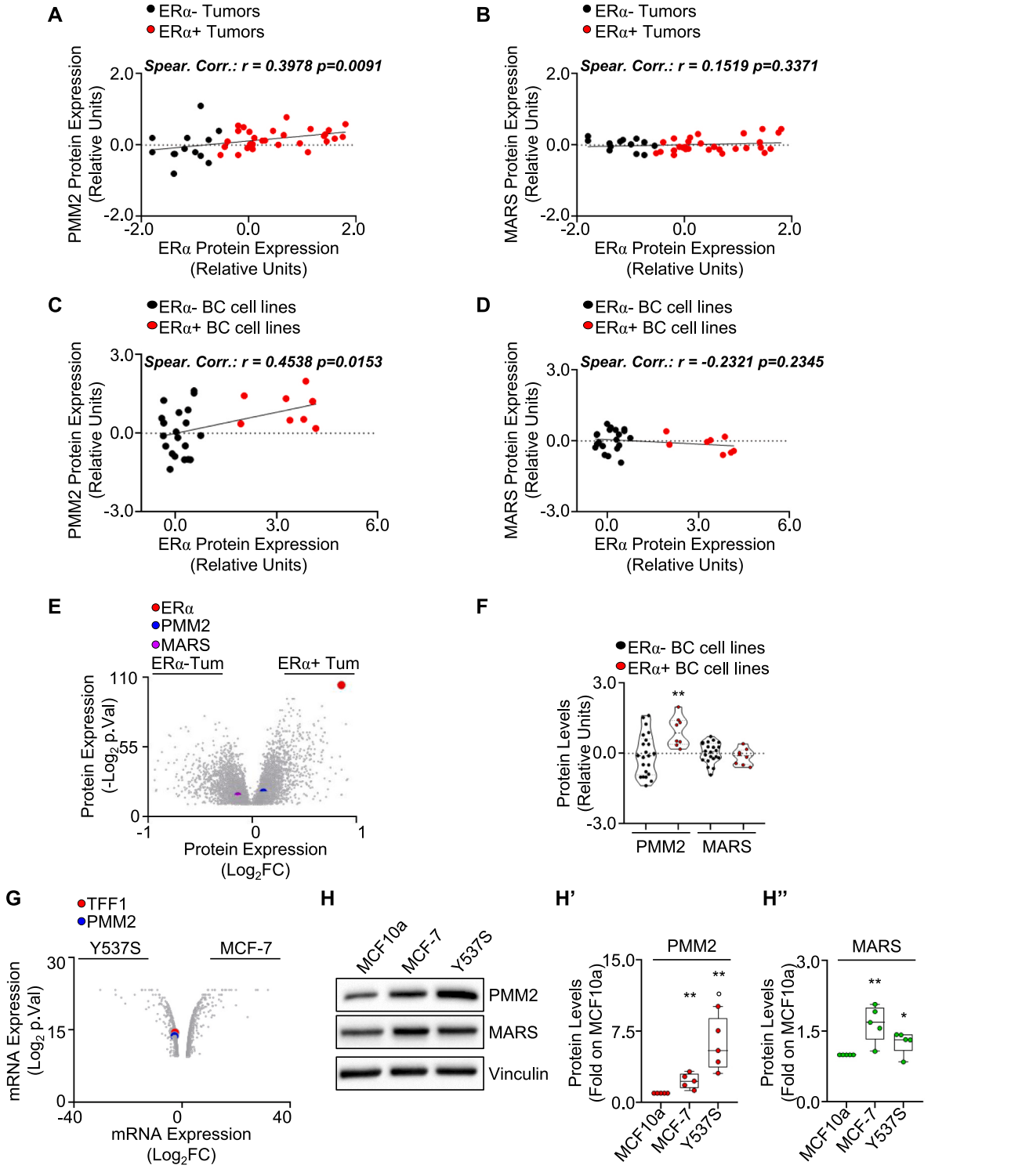

(caption on next page)

Fig. 3. The interaction among MARS, PMM2 and ERα-positive in breast tumors and in BC cells.
Correlation and regression analysis between ERα and PMM2 (A) or ERα and MARS (B) protein expression in ERα-negative (black dots) and ERα-positive (red dots) breast tumors obtained from the breast cancer landscape (Johansson et al., 2019) *via* the https://www.breastcancerlandscape.org/website. The main panel provides the correlation coefficient (r) and corresponding p-values. Each dot represents the protein expression value in a single tumor sample. Correlation and regression analysis between ERα and PMM2 (C) or ERα and MARS (D) protein expression in ERα-negative (black dots) and ERα-positive (red dots) breast cancer cell lines. The data were retrieved from the Broad Institute through the DepMap portal at https://depmap.org/portal. The main panel displays the correlation coefficient (r) and p-values. Each dot represents the protein expression value in a single breast cancer cell line. (E) Volcano plot illustrating the protein expression of ERα (red), PMM2 (blue), and MARS (purple) in ERα-negative or ERα-positive tumors, as provided by the breast cancer landscape (Johansson et al., 2019) and downloaded by https://www.breastcancerlandscape.org/. (F) PMM2 and MARS protein expression in ERα-negative (black dots) and ERα-positive (red dots) breast cancer cell lines. The data were obtained from the Broad Institute via the DepMap portal at https://depmap.org/portal. Each dot represents the protein expression value in a single breast cancer cell line. Significant differences compared to ERα-negative breast cancer cell lines were determined using unpaired two-tailed Student's t-test. The mean ± standard deviation is presented. ** $p < 0.01$. (G) Volcano plot showing the mRNA expression of TFF1 (red) and PMM2 (blue) in MCF-7 (FROM ATCC) or MCF-7-Y537S cells, as assessed by Affymetrix analysis described in our previous study (Busonero, 2018). Western blot analysis (H) and relative densitometric quantification (H′ and H″) of PMM2 and MARS expression levels in MCF-10a, MCF-7 (FROM ATCC), and MCF-7-Y537S cells. Vinculin expression served as the loading control on the same filter. Dots indicate the number of replicates. Significant differences compared to MCF-10a were determined using unpaired two-tailed Student's t-test. The mean ± standard deviation is presented. ** $p < 0.01$; * $p < 0.05$ compared to MCF-10a. ° $p < 0.05$ compared to MCF-7 (FROM ATCC). The number of replicates is indicated by solid dots in the bar graph.

expressing this particular receptor variant (Busonero et al., 2019). Promising approaches include the development of drugs that induce degradation of the ERα Y537S variant (e.g., AZD9496 - AZD and GDC-0810 - GDC) or target CDK4/CDK6 kinases (e.g., abemaciclib - Abe, palbociclib - Palbo, ribociclib - Ribo), which are now being utilized in clinical settings for managing this disease (Busonero et al., 2019; Katzenellenbogen et al., 2018).

Given our observation that PMM2 reduces ERα levels and inhibits the proliferation of MCF-7-Y537S cells, we aimed to investigate whether reducing PMM2 intracellular levels could enhance the anti-proliferative effects of the aforementioned drugs. To this end, we conducted growth curve analyses in both wt and PMM2 siRNA-depleted MCF-7-Y537S cells (Fig. 7A) in the presence or absence of Tam, ICI, AZD, GDC, Abe, Palbo, and Ribo. The effect of each drug was assessed when control cells reached 100% growth, and the cell number was determined using the normalized cell index (CI) (please refer to the Material and Methods section for detailed information). The results demonstrated that treatment with 10 μM of Tam, ICI, AZD, and GDC, as well as 1 μM of Abe, Palbo, and Ribo, did not significantly alter the proliferation of MCF-7-Y537S cells. In contrast, PMM2 depletion significantly reduced the normalized CI (Fig. 7B–D), as expected. Interestingly, we further observed that the administration of Tam, ICI, AZD, GDC, and Abe augmented the reduction in normalized CI induced by PMM2 depletion in MCF-7-Y537S cells (Fig. 7B–D).

These findings indicate that reducing PMM2 expression sensitizes MCF-7-Y537S cells to the anti-proliferative effects of both ET drugs and CDK4/CDK6 inhibitors.

4. Discussion

It is widely acknowledged that metabolic reprogramming is a hallmark of cancer (Pavlova and Thompson, 2016; Pavlova et al., 2022). The crucial adaptation of cancer cells lies in their ability to modify the utilization pathway of glucose, which is essential for sustaining cellular proliferation. Notably, it is noteworthy that various tumor types can remodel virtually all metabolic pathways (Pavlova and Thompson, 2016; Pavlova et al., 2022). The notion of metabolic reprogramming extends to BC, as diverse metabolic alterations can occur in various BC subtypes (Gandhi and Das, 2019). Recent findings from our research demonstrate the upregulation of glutamine levels in ERα-positive tumors, as well as the upregulation of the de novo purine biosynthetic pathway in luminal A ERα expressing ductal carcinoma (Cipolletti et al., 2023). These specific characteristics highlight potential novel targets for personalized treatment approaches in addressing this disease.

The therapeutic approach for ERα-positive BCs involves the administration of ET drugs such as aromatase inhibitors, 4OH-tamoxifen, and fulvestrant. These drugs have been recognized as effective anti-tumor treatments, and patients undergo prolonged treatment with them. However, a considerable proportion of women experience relapse, leading to the development of metastatic disease that becomes insensitive to ET drugs (Lumachi et al., 2011). Among the various mechanisms contributing to this resistance, there is growing evidence that specific point mutations in the ERα of BC cells emerge, promoting uncontrolled metastatic cell proliferation (Dustin et al., 2019; Pejerrey et al., 2018).

Numerous variants of ERα have been discovered, with the ERα Y537S mutation being the most prevalent and aggressive (Dustin et al., 2019). The ERα Y537S mutant exhibits diminished binding affinities for the ET drugs 4OH-tamoxifen and fulvestrant (Katzenellenbogen et al., 2018). Consequently, the clinical approach to targeting metastatic BC expressing this mutation involves developing new inhibitors of ERα that can facilitate its degradation (Katzenellenbogen et al., 2018). However, alternative strategies have emerged, as our recent research has identified FDA-approved drugs capable of inducing the degradation of ERα Y537S, thereby impeding the proliferation of cells expressing this receptor variant (Bartoloni et al., 2020, 2022; Busonero et al., 2017, 2018, 2020; Cipolletti et al., 2021a, 2023; Pescatori et al., 2022; Busonero, 2018). Based on the available evidence, a novel concept emerges suggesting that reducing receptor levels through the use of ET drugs alone or in combination with drugs targeting unrelated ERα pathways (e.g., CDK4/CDK6 inhibition) appears to be the most promising strategy for impeding the growth of metastatic BC that expresses ERα variants.

The molecular analysis of the ERα Y537S mutant in cells reveals that the emergence of this mutation is accompanied by a metabolic reprogramming in mitochondrial and lipid pathways (Fiorillo et al., 2018; Martin et al., 2017; Du et al., 2018). Consequently, we conducted a siRNA-based screen to identify metabolic proteins capable of reducing intracellular levels of the ERα Y537S variant in metastatic BC (Cipolletti et al., 2023). These identified proteins hold potential as novel targets for the treatment of this specific disease. Out of the nine metabolic proteins identified in the screen for inducing ERα degradation and inhibiting cell proliferation specifically in cells expressing the ERα Y537S mutant, our focus turned to PMM2. This choice was driven by several factors: i) PMM2 exhibited lower mRNA levels that correlated with a better relapse free survival (RFS) rate in women with ERα-positive BC; ii) it was found to be overexpressed in high-grade and advanced-stage ERα-positive tumors; and iii) it showed higher expression in ERα-positive cell lines compared to ERα-negative tumors and cell lines. Moreover, noteworthy is the observation that both PMM2 mRNA and protein levels were found to be elevated in ductal carcinoma cells expressing the ERα Y537S variant. Accordingly, we present significant findings indicating that depletion of PMM2 has a preferential ability to induce degradation of the ERα Y537S variant and effectively inhibit cell proliferation in its expressing cells. Furthermore, the reduction of PMM2 levels in these cells effectively inhibits the hyperactive signaling of the ERα Y537S variant by diminishing both its ERE-based transcriptional activity and the expression of E2-target genes. Notably, our growth curve studies

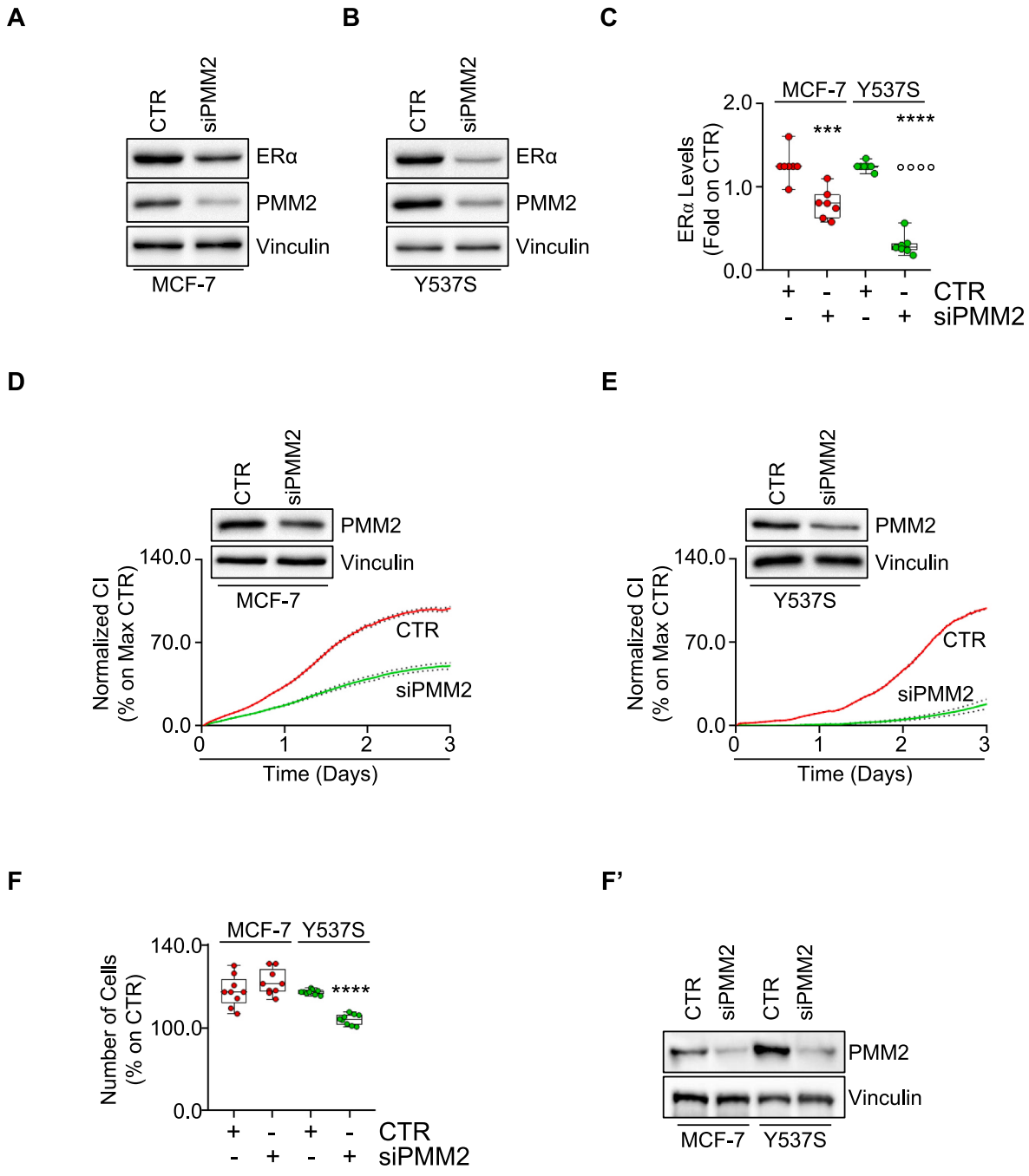

Fig. 4. The impact of PMM2 in the regulation of ERα levels and cell proliferation.
Western blot analysis (A and B) and relative densitometric quantification (C) of ERα expression levels in MCF-7 (FROM ATCC) (A) and MCF-7-Y537S cells (B) with or without treatment with siRNA targeting PMM2. Vinculin expression was used as the loading control on the same blot. Significant differences compared to control samples (CTR) were determined using unpaired two-tailed Student's t-test. The mean ± standard deviation is shown. *** $p < 0.001$; **** $p < 0.0001$ compared to CTR. °°°° $p < 0.0001$ compared to PMM2 siRNA in MCF-7 (FROM ATCC). The number of replicates is indicated by solid dots in the bar graph. Growth curve analyses of MCF-7 (FROM ATCC) (D) and MCF-7-Y537S (E) cells were conducted according to the methods described in the Materials and Methods section for 3 days following transfection with siRNA oligonucleotides targeting PMM2. The graphs display the normalized cell index (representing cell number), which was measured using the xCelligence DP device and calculated relative to the control sample at each time point. Each sample was measured in quadruplicate. Insets in panels D and E present controls for the PMM2 siRNA experiments. The experiment was repeated twice in duplicate, and the curves represent the mean values ± the standard deviation, which is indicated as the dotted line above and below the curves. Further information can be found in the Materials and Methods section. (F) Number of MCF-7 (FROM ATCC) and MCF-7-Y537S cells measured with the Crystal Violet method (please see the Materials and Methods section) 3 days following transfection with siRNA oligonucleotides targeting PMM2. Significant differences compared to control samples (CTR) were determined using unpaired two-tailed Student's t-test. The mean ± standard deviation is shown. **** $p < 0.0001$ compared to CTR. Dots indicate the number of replicates. (F') Control Western blot analyses of PMM2 and vinculin levels measured 3 days following transfection with siRNA oligonucleotides targeting PMM2.

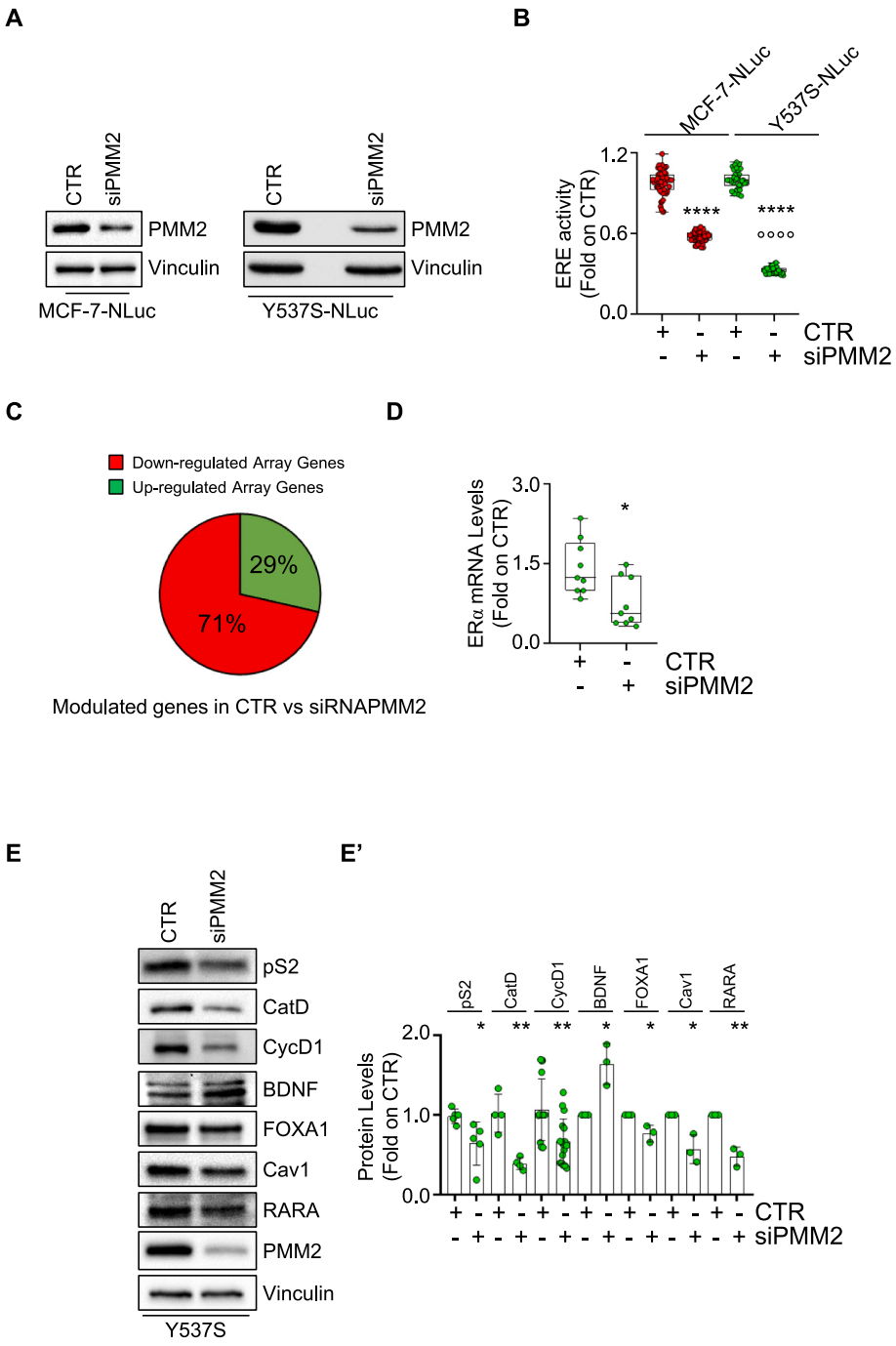

Fig. 5. The impact of PMM2 in ERα Y537S variant E2-dependent transcriptional activity and gene expression.
(A) Western blot analysis depicting PMM2 expression levels in MCF-7 (right) and MCF-7-Y537S estrogen response element (ERE)-NLuc cells (left) (Cipolletti et al., 2020, 2021b). Vinculin expression served as the loading control on the same filter. (B) Estrogen response element (ERE) promoter activity in MCF-7 and MCF-7-Y537S ERE-NLuc cells (Cipolletti et al., 2020, 2021b) following siRNA-mediated depletion of PMM2. The experiments were conducted three times with quintuplicate samples. Significant differences were assessed using the unpaired two-tailed Student's t-test. **** (p-value <0.0001) denotes significant differences compared to the control (CTR) sample in each cell line. ° (p-value <0.0001) denotes significant differences between the PMM2 siRNA in MCF-7 and MCF-7-Y537S ERENluc cells. Dots indicate the number of replicates. (C) Pie diagrams illustrating the percentages of modulated array genes in MCF-7-Y537S cells treated with siRNA targeting PMM2. The thresholds for gene modulation are indicated in the main figures. The experiments were repeated twice. (D) mRNA levels in MCF-7-Y537S cells following siRNA-mediated depletion of PMM2. * (p-value <0.05) indicates significant differences compared to the control (CTR) sample. Dots represent the number of replicates. Western blot analysis (E) and relative densitometric quantification (E′) of presenilin 2 (pS2), cathepsin D (CatD), cyclin D1 (CycD1), brain-derived neurotrophic factor (BDNF), FOXA1, caveolin-1 (Cav1), retinoic acid receptor alpha (RARA), and PMM2 expression levels in MCF-7-Y537S cells with or without siRNA targeting PMM2. Vinculin expression was used as the loading control on the same blot. Significant differences compared to the control (CTR) samples were determined using unpaired two-tailed Student's t-test. The mean ± standard deviation is presented. * $p < 0.05$; ** $p < 0.01$ compared to CTR. The number of replicates is indicated by solid dots in the bar graph.

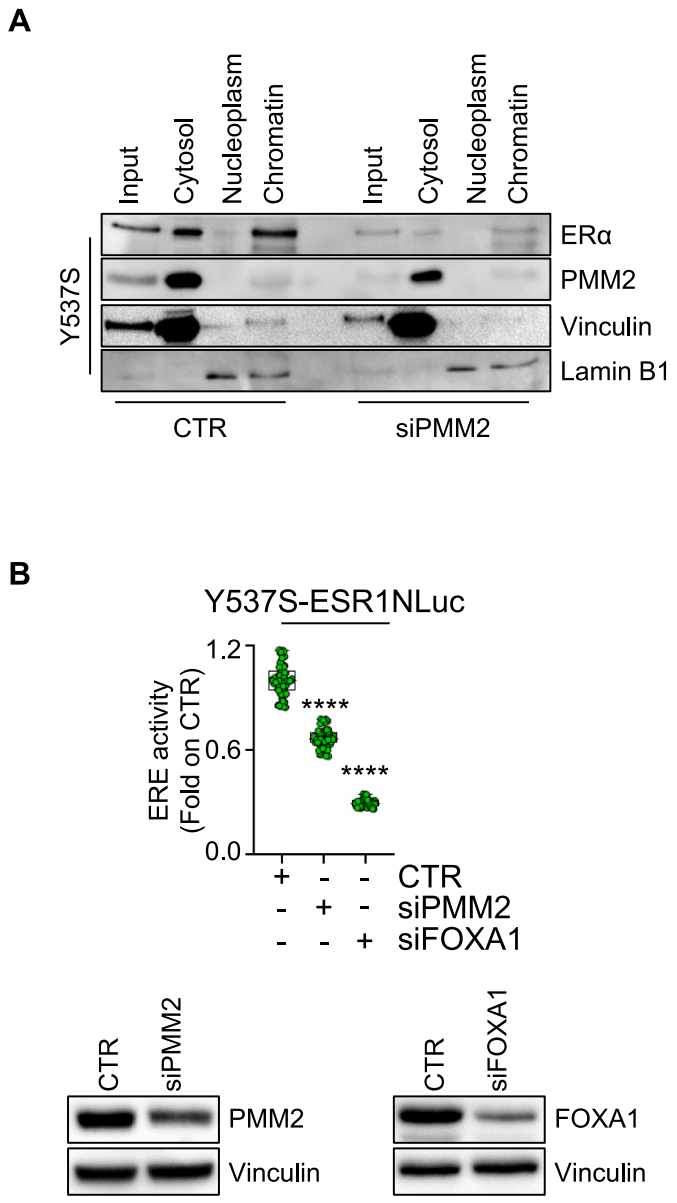

Fig. 6. The impact of PMM2 in ERα recruitment on the chromatin and in FOXA1-dependent regulation of ERα promoter activation.
(A) Western blot analysis depicting the levels of ERα, PMM2 vinculin, and lamib B1 in MCF-7-Y537S in the presence and the absence of the siRNA-mediated depletion of PMM2. The experiments have been performed in triplicate and the figure shows representative blots. (B) FOXA1-dependent activity of the enhancer located in the *ESR1* gene promoter in MCF-7-Y537S ESR1-NLuc cells generated as reported in (Bartoloni et al., 2022) following siRNA-mediated depletion of PMM2 and FOXA1. The experiments were conducted twice with sextuplicate samples. Significant differences were assessed using the unpaired two-tailed Student's t-test. **** (p-value <0.0001) denotes significant differences compared to the control (CTR) sample in each cell line. Dots indicate the number of replicates.

demonstrate that reducing PMM2 levels re-sensitizes ERα Y537S-expressing cells to certain ET drugs and CDK4/CDK6 inhibitors. Particularly interesting is the combinatorial effect of ET drugs, which induce receptor degradation, and CDK4/CDK6 inhibitors. Targeting PMM2 to reduce ERα levels, and concurrently utilizing either drugs to further degrade the receptor or block a pathway parallel to receptor degradation, aligns perfectly with the concept of targeting multiple pathways to impede the growth of metastatic BC expressing the ERα Y537S variant.

From a mechanistic perspective, our observations indicate that depletion of PMM2 leads to a reduction in *ESR1* mRNA levels, consequently resulting in decreased expression of the ERα receptor protein. Notably, we also observed that PMM2 reduction causes a decrease in FOXA1 mRNA and protein levels. FOXA1 serves as a pioneering factor for ERα and transcriptionally regulates its expression (Bernardo et al., 2010). Moreover, we have shown that the reduction of ERα Y537S depends on the siRNA-induced reduction of FOXA1 mediated by PMM2. Indeed, under these conditions, the ability of FOXA1 to control the activity of its enhancer on the *ESR1* gene promoter region is strongly impaired.

Regarding the mechanism through which PMM2 affects the stability of FOXA1, it is important to point out that PMM2 is the phosphomannose mutase 2, an enzyme that catalyzes the isomerization of mannose-6-phosphate to mannose-1-phosphate, which is essential for the synthesis of dolichol-P-oligosaccharides (Lam and Krasnewich, 1993). These compounds play a crucial role in protein glycosylation, and mutations in the PMM2 gene are associated with congenital disorders of glycosylation (Lam and Krasnewich, 1993). Interestingly, it has been demonstrated that FOXA1 undergoes glycosylation, which regulates its stability (Niang et al., 2016). Therefore, it is plausible that in ERα Y537S expressing cells, depletion of PMM2 would reduce FOXA1 glycosylation, leading to a decrease in FOXA1 protein levels. This reduction in FOXA1 subsequently contributes to a decrease in intracellular levels of the mutant ERα.

Currently, there are no available PMM2 inhibitors; however, our observations suggest the possibility of utilizing such drugs for the treatment of metastatic BC. Additionally, it is tempting to speculate that inhibitors of glycosylation could be employed as a potential treatment for ERα Y537S mutant expressing metastatic BC. These inhibitors could induce receptor degradation, thereby blocking cell proliferation. This speculation is particularly intriguing given the growing interest in enzymes involved in glycosylation pathways as novel therapeutic targets in BC (Peric et al., 2022).

In conclusion, our findings establish PMM2 as a promising and innovative therapeutic target for addressing metastatic BC characterized by the presence of the ERα Y537S variant. These results offer potential alternative strategies for managing and treating this disease, broadening the therapeutic options available.

Ethics approval

'Not applicable'.

Funding

The research leading to these results has received funding from AIRC under IG 2018 - ID. 21325 project – P.I. Acconcia Filippo. This study was also supported by grants from Ateneo Roma Tre to FA. The Grant of Excellence Departments, MIUR (ARTICOLO 1, COMMI 314–337 LEGGE 232/2016) to the Department of Science, University Roma TRE and Rome Technopole are also gratefully acknowledged.

Availability of data and materials

All the original Western blots and the original data for synergy proliferation experiments are available from the corresponding author on reasonable request.

All the Kaplan-Meier curves were retrieved from the Kaplan-Meier Plotter database and given in Supplementary Table 1 as downloaded by the website (https://kmplot.com/analysis/) (Lanczky and Gyorffy, 2021). All the datasets used to generate Fig. 2C, D and 2F were downloaded by the Broad Institute through the DepMap portal (https://depmap.org/portal) and are available in Supplementary Table 6. The original data for Fig. 1E were downloaded by the TNMplot: differential gene expression analysis in Tumor, Normal, and Metastatic tissues

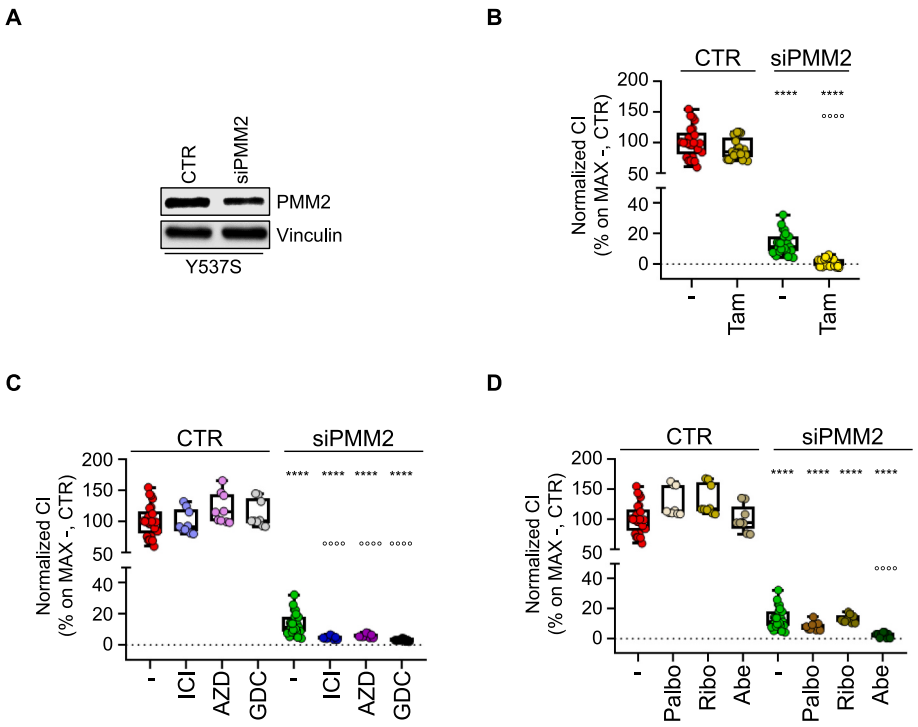

Fig. 7. PMM2 synergic effects with clinically relevant drugs used to treat metastatic BC.
(A) Western blot analysis depicting PMM2 expression levels in MCF-7-Y537S following siRNA-mediated depletion of PMM2. Vinculin expression served as the loading control on the same filter.
Growth curves of MCF-7-Y537S cells treated with or without siRNA targeting PMM2, along with 4OH-Tamoxifen (Tam - 10 μM) (B), fulvestrant (ICI182,280 - ICI 10 μM) (C), AZD (AZD 10 μM) (C), GDC (GDC 10 μM) (C), abemaciclib (Abe 1 μM) (D), palbociclib (Palbo 1 μM) (D), ribociclib (Ribo 1 μM) (D). The data are presented as a percentage of the maximum effect observed in the growth curve of the untreated samples. Significant differences compared to the control (CTR) samples were determined using the unpaired two-tailed Student's t-test and denoted as **** p-value <0.0001. Significant differences between the cells treated with siRNA for PMM2 alone and those treated with siRNA for PMM2 in combination with the different drugs were calculated using the unpaired two-tailed Student's t-test and indicated as °°°° p-value <0.0001. Dots indicate the number of replicates. For further details, please refer to the Materials and Methods section.

(TNMplot) (https://tnmplot.com/analysis/) database and given in Supplementary Table 2. The original data for Fig. 1F were downloaded by cbioportal.org and given in Supplementary Table 3 and Table 4.

The original numbers in Fig. 2G are available in Supplementary Table 4 and have been extracted from the supplementary materials given in (Finlay-Schultz et al., 2020). The datasets for Fig. 2E and those used to generate Fig. 2A and B have been downloaded by the breast cancer landscape website (https://www.breastcancerlandscape.org/) as associated with the paper published in (Johansson et al., 2019). Original data for Fig. 2A and B are given also in Supplementary Table 5. Data for the generation of Fig. 2G are given in Supplementary Table 7 as extracted by our previous work (Busonero, 2018).

CRediT authorship contribution statement

Manuela Cipolletti: Conceptualization, Formal analysis, Investigation, Methodology, Writing – review & editing. **Filippo Acconcia:** Conceptualization, Formal analysis, Funding acquisition, Investigation, Supervision, Writing – original draft, Writing – review & editing.

Declaration of generative AI and AI-assisted technologies in the writing process

During the preparation of this work the author(s) used ChatGPT in order to improve language and readability. After using this tool, the author(s) reviewed and edited the content as needed and take(s) full responsibility for the content of the publication.

Declaration of competing interest

None.

Data availability

I have inserted this information in the main text

Acknowledgments

The research leading to these results has received funding from AIRC under IG 2018 - ID. 21325 project – P.I. Acconcia Filippo. This study was also supported by grants from Ateneo Roma Tre to FA. The Grant of Excellence Departments, MIUR (ARTICOLO 1, COMMI 314–337 LEGGE 232/2016) to the Department of Science, University Roma TRE is also gratefully acknowledged. The authors are grateful to Prof. Simak Ali, University of London Imperial College for the gift of the MCF-7 Y537S cells.

Appendix A. Supplementary data

Supplementary data to this article can be found online at https://doi.org/10.1016/j.mce.2024.112160.

List of abbreviations

Abe	Abemaciclib
AZD	AZD9496
AZIN2	Arginine Decarboxylase
BC	breast cancer

BDNF	Brain Derived Neurotrophic Factor
CA14	Carbonic anhydrase 14
CA4	Carbonic anhydrase 4
CatD	cathepsin D
Cav1	caveolin-1
CDK4	cyclin-dependent kinase 4
CDK6	cyclin-dependent kinase 6
CycD1	cyclin D1
DMEM	Dulbecco's Midified Eagle Medium
E2	17β-estradiol
ERE	estrogen responsive element
ERα	estrogen receptor α
ET	Endocrine therapy
FDA	Food and Drug Administration
FKBP6	FKBP Prolyl Isomerase Family Member 6 (Inactive)
FOXA1	Forkhead Box A1
GAD1	Glutamate Decarboxylase 1
GART	Phosphoribosylglycinamide Formyltransferase, Phosphoribosylglycinamide Synthetase, Phosphoribosylaminoimidazole Synthetase
GDC	GDC-0810
HER2	Human Epidermal Growth Factor Receptor 2
MARS	Methionyl-TRNA Synthetase 1
Palbo	Palbociclib
PGAM2	Phosphoglycerate Mutase 2
PMM2	Phosphomannomutase 2
pS2	presenelin2
RARA	retinoic acid receptor alpha
RFS	relapse free survival
Ribo	Ribociclib
SLC27A4	Solute Carrier Family 27 Member 4
Tam	4OH-tamoxifen
TFF1	trefoil factor 1
YY	Buffer: Yoss Yarden Buffer

References

Acconcia, F., Barnes, C.J., Singh, R.R., Talukder, A.H., Kumar, R., 2007. Proceedings of the National Academy of Sciences of the United States of America 104, 6782–6787. https://doi.org/10.1073/pnas.0701999104.

Acconcia, F., Fiocchetti, M., Busonero, C., Fernandez, V.S., Montalesi, E., Cipolletti, M., Pallottini, V., Marino, M., 2021. Mol. Cell. Endocrinol. 538, 111452. https://doi.org/10.1016/j.mce.2021.111452.

Bartha, A., Gyorffy, B., 2021. International journal of molecular sciences 22. https://doi.org/10.3390/ijms22052622.

Bartoloni, S., Leone, S., Acconcia, F., 2020. International journal of molecular sciences 21. https://doi.org/10.3390/ijms21103418.

Bartoloni, S., Leone, S., Pescatori, S., Cipolletti, M., Acconcia, F., 2022. Mol. Oncol. 16, 3568–3584. https://doi.org/10.1002/1878-0261.13303.

Bernardo, G.M., Lozada, K.L., Miedler, J.D., Harburg, G., Hewitt, S.C., Mosley, J.D., Godwin, A.K., Korach, K.S., Visvader, J.E., Kaestner, K.H., Abdul-Karim, F.W., Montano, M.M., Keri, R.A., 2010. Development 137, 2045–2054. https://doi.org/10.1242/dev.043299.

Busonero, C.L., S.; Bianchi, F.; Acconcia, F., 2018. Cellular oncology. https://doi.org/10.1007/s13402-018-0400-x.

Busonero, C., Leone, S., Acconcia, F., 2017. Cell. Oncol. https://doi.org/10.1007/s13402-017-0322-z.

Busonero, C., Leone, S., Klemm, C., Acconcia, F., 2018. Mol. Cell. Endocrinol. 460, 229–237. https://doi.org/10.1016/j.mce.2017.07.027.

Busonero, C., Leone, S., Bartoloni, S., Acconcia, F., 2019. Mol. Cell. Endocrinol. 480, 107–121. https://doi.org/10.1016/j.mce.2018.10.020.

Busonero, C., Leone, S., Bianchi, F., Maspero, E., Fiocchetti, M., Palumbo, O., Cipolletti, M., Bartoloni, S., Acconcia, F., 2020. Cancers (Basel) 12. https://doi.org/10.3390/cancers12123840.

Cerami, E., Gao, J., Dogrusoz, U., Gross, B.E., Sumer, S.O., Aksoy, B.A., Jacobsen, A., Byrne, C.J., Heuer, M.L., Larsson, E., Antipin, Y., Reva, B., Goldberg, A.P., Sander, C., Schultz, N., 2012. Cancer Discov. 2, 401–404. https://doi.org/10.1158/2159-8290.CD-12-0095.

Cipolletti, M., Leone, S., Bartoloni, S., Busonero, C., Acconcia, F., 2020. J. Cell. Physiol. https://doi.org/10.1002/jcp.29565.

Cipolletti, M., Bartoloni, S., Busonero, C., Parente, M., Leone, S., Acconcia, F., 2021a. International journal of molecular sciences 22. https://doi.org/10.3390/ijms22062915.

Cipolletti, M., Pescatori, S., Acconcia, F., 2021b. Endocrine 2, 54–64. https://doi.org/10.3390/endocrines2010006.

Cipolletti, M., Leone, S., Bartoloni, S., Acconcia, F., 2023. Front. Endocrinol. 14, 1129162. https://doi.org/10.3389/fendo.2023.1129162.

Curtis, C., Shah, S.P., Chin, S.F., Turashvili, G., Rueda, O.M., Dunning, M.J., Speed, D., Lynch, A.G., Samarajiwa, S., Yuan, Y., Graf, S., Ha, G., Haffari, G., Bashashati, A., Russell, R., McKinney, S., Group, M., Langerod, A., Green, A., Provenzano, E., Wishart, G., Pinder, S., Watson, P., Markowetz, F., Murphy, L., Ellis, I., Purushotham, A., Borresen-Dale, A.L., Brenton, J.D., Tavare, S., Caldas, C., Aparicio, S., 2012. Nature 486, 346–352. https://doi.org/10.1038/nature10983.

Dai, X., Cheng, H., Bai, Z., Li, J., 2017. J. Cancer 8, 3131–3141. https://doi.org/10.7150/jca.18457.

Du, T., Sikora, M.J., Levine, K.M., Tasdemir, N., Riggins, R.B., Wendell, S.G., Van Houten, B., Oesterreich, S., 2018. Breast cancer research. BCR 20, 106. https://doi.org/10.1186/s13058-018-1041-8.

Dustin, D., Gu, G., Fuqua, S.A.W., 2019. Cancer 125, 3714–3728. https://doi.org/10.1002/cncr.32345.

Finlay-Schultz, J., Jacobsen, B.M., Riley, D., Paul, K.V., Turner, S., Ferreira-Gonzalez, A., Harrell, J.C., Kabos, P., Sartorius, C.A., 2020. Breast cancer research. BCR 22, 68. https://doi.org/10.1186/s13058-020-01300-y.

Fiorillo, M., Sanchez-Alvarez, R., Sotgia, F., Lisanti, M.P., 2018. Aging (Albany NY) 10, 4000–4023. https://doi.org/10.18632/aging.101690.

Gandhi, N., Das, G.M., 2019. Cells 8. https://doi.org/10.3390/cells8020089.

Gao, J., Aksoy, B.A., Dogrusoz, U., Dresdner, G., Gross, B., Sumer, S.O., Sun, Y., Jacobsen, A., Sinha, R., Larsson, E., Cerami, E., Sander, C., Schultz, N., 2013. Sci Signal 6, pl1. https://doi.org/10.1126/scisignal.2004088.

Harrod, A., Fulton, J., Nguyen, V.T.M., Periyasamy, M., Ramos-Garcia, L., Lai, C.F., Metodieva, G., de Giorgio, A., Williams, R.L., Santos, D.B., Gomez, P.J., Lin, M.L., Metodiev, M.V., Stebbing, J., Castellano, L., Magnani, L., Coombes, R.C., Buluwela, L., Ali, S., 2017. Oncogene 36, 2286–2296. https://doi.org/10.1038/onc.2016.382.

Harrod, A., Lai, C.F., Goldsbrough, I., Simmons, G.M., Oppermans, N., Santos, D.B., Gyorffy, B., Allsopp, R.C., Toghill, B.J., Balachandran, K., Lawson, M., Morrow, C.J., Surakala, M., Carnevalli, L.S., Zhang, P., Guttery, D.S., Shaw, J.A., Coombes, R.C., Buluwela, L., Ali, S., 2022. Oncogene 41, 4905–4915. https://doi.org/10.1038/s41388-022-02483-8.

Johansson, H.J., Socciarelli, F., Vacanti, N.M., Haugen, M.H., Zhu, Y., Siavelis, I., Fernandez-Woodbridge, A., Aure, M.R., Sennblad, B., Vesterlund, M., Branca, R.M., Orre, L.M., Huss, M., Fredlund, E., Beraki, E., Garred, O., Boekel, J., Sauer, T., Zhao, W., Nord, S., Hoglander, E.K., Jans, D.C., Brismar, H., Haukaas, T.H., Bathen, T.F., Schlichting, E., Naume, B., Consortia Oslo Breast Cancer Research, C., Luders, T., Borgen, E., Kristensen, V.N., Russnes, H.G., Lingjaerde, O.C., Mills, G.B., Sahlberg, K.K., Borresen-Dale, A.L., Lehtio, J., 2019. Nat. Commun. 10, 1600. https://doi.org/10.1038/s41467-019-09018-y.

Katzenellenbogen, J.A., Mayne, C.G., Katzenellenbogen, B.S., Greene, G.L., Chandarlapaty, S., 2018. Nat. Rev. Cancer 18, 377–388. https://doi.org/10.1038/s41568-018-0001-z.

Lam, C., Krasnewich, D.M., 1993. in GeneReviews((R)), ed. by M.P. Adam, G.M. Mirzaa, R.A. Pagon, S.E. Wallace, L.J.H. Bean, K.W. Gripp and A. Amemiya (Seattle (WA).

Lanczky, A., Gyorffy, B., 2021. J. Med. Internet Res. 23, e27633 https://doi.org/10.2196/27633.

Lumachi, F., Luisetto, G., Basso, S.M., Basso, U., Brunello, A., Camozzi, V., 2011. Curr. Med. Chem. 18, 513–522. PMID: 21143113.

Martin, L.A., Ribas, R., Simigdala, N., Schuster, E., Pancholi, S., Tenev, T., Gellert, P., Buluwela, L., Harrod, A., Thornhill, A., Nikitorowicz-Buniak, J., Bhamra, A., Turgeon, M.O., Poulogiannis, G., Gao, Q., Martins, V., Hills, M., Garcia-Murillas, I., Fribbens, C., Patani, N., Li, Z., Sikora, M.J., Turner, N., Zwart, W., Oesterreich, S., Carroll, J., Ali, S., Dowsett, M., 2017. Nat. Commun. 8, 1865. https://doi.org/10.1038/s41467-017-01864-y.

Neve, R.M., Chin, K., Fridlyand, J., Yeh, J., Baehner, F.L., Fevr, T., Clark, L., Bayani, N., Coppe, J.P., Tong, F., Speed, T., Spellman, P.T., DeVries, S., Lapuk, A., Wang, N.J., Kuo, W.L., Stilwell, J.L., Pinkel, D., Albertson, D.G., Waldman, F.M., McCormick, F., Dickson, R.B., Johnson, M.D., Lippman, M., Ethier, S., Gazdar, A., Gray, J.W., 2006. Cancer Cell 10, 515–527. https://doi.org/10.1016/j.ccr.2006.10.008.

Niang, B., Jin, L., Chen, X., Guo, X., Zhang, H., Wu, Q., Padhiar, A.A., Xiao, M., Fang, D., Zhang, J., 2016. Mol. Cell. Biochem. 411, 393–402. https://doi.org/10.1007/s11010-015-2601-1.

Pavlova, N.N., Thompson, C.B., 2016. Cell Metabol. 23, 27–47. https://doi.org/10.1016/j.cmet.2015.12.006.

Pavlova, N.N., Zhu, J., Thompson, C.B., 2022. Cell Metabol. 34, 355–377. https://doi.org/10.1016/j.cmet.2022.01.007.

Pejerrey, S.M., Dustin, D., Kim, J.A., Gu, G., Rechoum, Y., Fuqua, S.A.W., 2018. Hormones & cancer. https://doi.org/10.1007/s12672-017-0306-5.

Peric, L., Vukadin, S., Petrovic, A., Kuna, L., Puseljic, N., Sikora, R., Rozac, K., Vcev, A., Smolic, M., 2022. Biomedicines 10. https://doi.org/10.3390/biomedicines10123265.

Pescatori, S., Leone, S., Cipolletti, M., Bartoloni, S., di Masi, A., Acconcia, F., 2022. J. Exp. Clin. Cancer Res. 41, 27. https://doi.org/10.1186/s13046-022-02360-y.

Soule, H.D., Maloney, T.M., Wolman, S.R., Peterson Jr., W.D., Brenz, R., McGrath, C.M., Russo, J., Pauley, R.J., Jones, R.F., Brooks, S.C., 1990. Cancer Res. 50, 6075–6086.

Tsang, J.Y.S., Tse, G.M., 2020. Adv. Anat. Pathol. 27, 27–35. https://doi.org/10.1097/PAP.0000000000000232.

Wang, D., Ren, J., Ren, H., Fu, J.L., Yu, D., 2018. Acta Pharmacol. Sin. 39, 124–131. https://doi.org/10.1038/aps.2017.89.